OAK RIDGE NATIONAL LABORATORY
operated by
UNION CARBIDE CORPORATION
NUCLEAR DIVISION
for the
U.S. ATOMIC ENERGY COMMISSION

MASTER

UNION
CARBIDE

FRACTIONAL CRYSTALLIZATION REACTIONS IN THE SYSTEM LiF-BeF$_2$-ThF$_4$

R. E. Thoma and J. E. Ricci[1]

ABSTRACT

Equilibrium and non-equilibrium crystallization reactions in the system
LiF-BeF$_2$-ThF$_4$ are analyzed in relation to their potential application to
molten salt reactor fuel reprocessing. Heterogeneous equilibria in the
temperature range from the liquidus at 590°C to the solidus at 350°C are
described quantitatively and in detail by means of ten typical isothermal
sections and by three temperature-composition sections. The implications
of metastable fractionation in this temperature interval are discussed
as a possible feed control step in reductive extraction reprocessing of
molten salt breeder reactor fuels.

CONTENTS

INTRODUCTION

The ORNL Molten Salt Reactor Program is devoted to the development of molten salt breeder reactors which employ mixtures of molten fluorides as core fluids. Until recently, the most promising approach to the development of molten salt breeder reactors appeared to be a two-region reactor with fissile and fertile materials in separate fuel and blanket streams. Thorium would be carried in the blanket salt, in a salt stream which would consist of a ^7LiF-BeF_2-ThF_4 mixture. Advances in chemical reprocessing have provided evidence recently that ^{233}Pa and possibly the rare earth fission products can be separated from mixed thorium-uranium salt by reductive extraction methods employing liquid bismuth. This development, along with other design developments, makes possible a single-fluid breeder reactor, one which has greater simplicity and reliability than the two-fluid reactor. The fuel for the single fluid reactor would be composed of ^7LiF, BeF_2, ThF_4, and $^{233}UF_4$, and might be expected to contain ~ 12 mole % ThF_4. Optimization of the ^7LiF and BeF_2 concentrations is not complete, because the trade-off values of several significant factors have not yet been established. These include selection limitations imposed by the equilibrium phase behavior of the LiF-BeF_2-ThF_4 system ($^{233}UF_4$ concentration will be only 0.2 mole %, and is therefore of little consequence in this connection), physical properties such as viscosity, vapor pressure, thermal conductivity, and the relations of LiF-BeF_2-ThF_4 composition to the development of chemical processes for removal of protactinium and the lanthanides.

Effective separation of the rare earth fission products from fluoride salt streams which contain thorium fluoride is the keystone to development of semi-continuous reprocessing in single-fluid molten salt reactors. Several methods for reprocessing spent LiF-BeF_2-ThF_4-UF_4 fuels are currently under investigation. The method which is regarded as most tractable for engineering development involves the selective chemical reduction of the various components into liquid bismuth solutions at about 600^0C, utilizing multistage countercurrent extraction operations. The current status of engineering development of this process has been described by Whatley et al.[2] The initial steps remove uranium and protactinium by reductive extraction.[3] A strong incentive then exists to remove the rare-earth fission products from the remaining salt. The most nearly feasible approach to this separation seems to be their extraction

into bismuth alloy,[3] even though the recycle volumes of extractant are marginally acceptable. The efficiency of this separation step would be greatly enhanced if the concentration of the rare earths in the salt mixture were increased by at least tenfold, and if the residual salt solutions were of a much lower concentration of thorium fluoride. That the $LiF-BeF_2-ThF_4$ phase diagram[4] shows the occurrence of low melting mixtures of low thorium fluoride content which are producible from MSBR single-core fluids by metastable crystallization has suggested the possibility that non-equilibrium fractionation reactions might be exploited as a feed control step in the reductive extraction process.

Because of its relative complexity, the unpublished version of the $LiF-BeF_2-ThF_4$ phase diagram may experience less frequent or less effective application in molten salt reactor technology than is warranted by the developments cited above. We therefore describe in this report further detailed aspects of equilibrium and non-equilibrium behavior in the system.

LIQUID-SOLID PHASE REACTIONS IN THE SYSTEM $LiF-BeF_2-ThF_4$

Methods for interpreting polythermal and isothermal phase diagrams are described extensively in an earlier report[5] where the phase relationships in a number of fluoride systems were analyzed in detail. Interpretation of the equilibrium behavior in the system $LiF-BeF_2-ThF_4$[4] (Figure 1) is somewhat more complex than for the systems analyzed because of the occurrence of an unusual solid solution which is produced as the compound $3LiF \cdot ThF_4$ crystallizes from $LiF-BeF_2-ThF_4$ melts. The crystal phase of nominal composition, $3LiF \cdot ThF_4$, precipitates as a ternary solid solution which, at its maximum in composition variability (near the solidus), is described by a composition triangle with apices at $LiF-ThF_4$ (75-25 mole %), $LiF-BeF_2-ThF_4$ (58-16-26 mole %), and $LiF-BeF_2-ThF_4$ (59-20-21 mole %). Two substitution models may provide an explanation for the single phase solid solution area: (1) a substitution of one Be^{2+} ion for a Li^+ ion with the simultaneous formation of a Th^{4+} vacancy for every four Be^{2+} ions substituted for Li^+ ions to provide electroneutrality and (2) substitution of a single Be^{2+} ion for a Li^+ ion with the simultaneous formation of a Li^+ vacancy. Model (1) would afford a solid solution
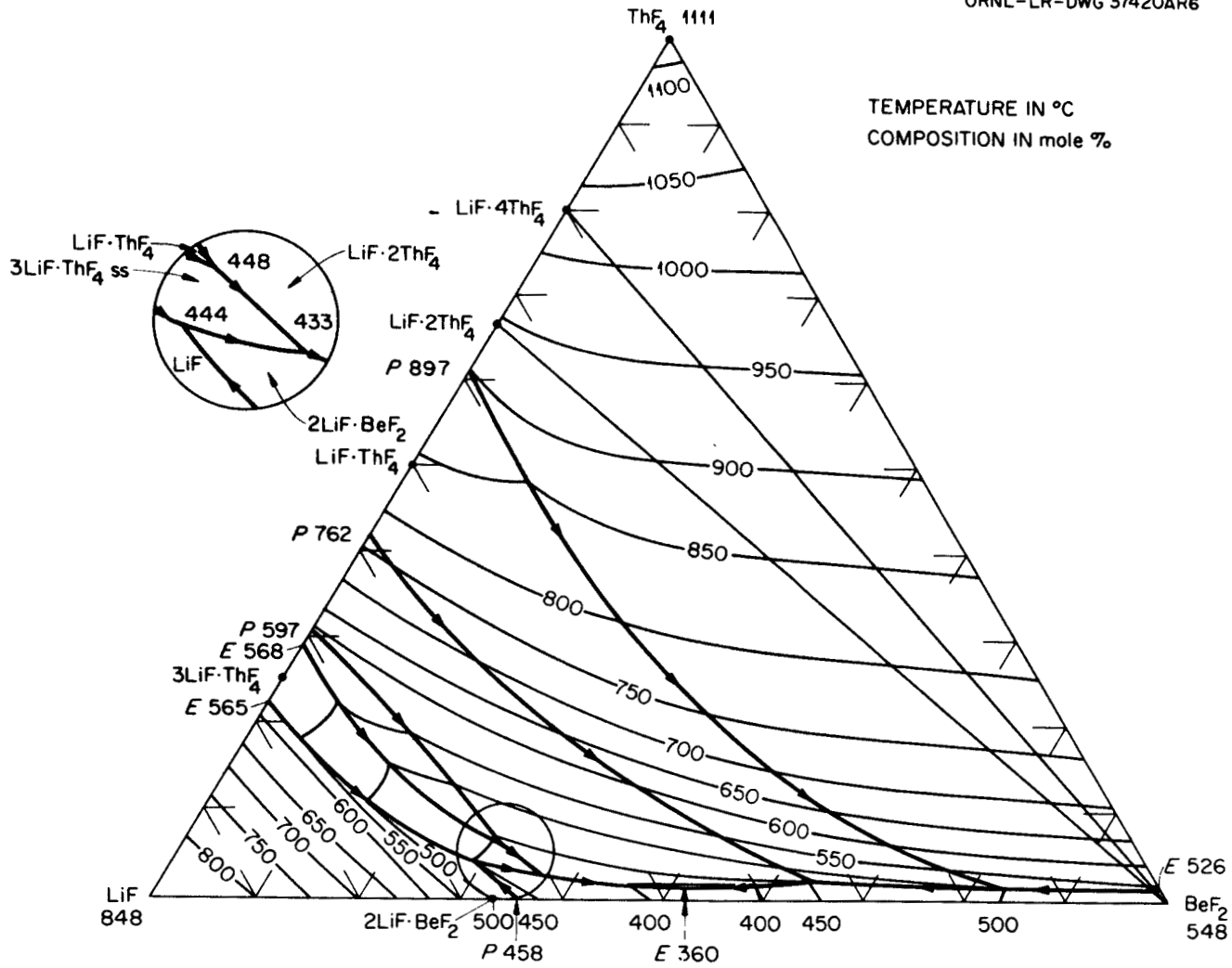
Fig. 1. Polythermal Projection of the $LiF-BeF_2-ThF_4$ Equilibrium Phase Diagram.

limit in good agreement with the leg of the triangular area with the lesser ThF_4 content whereas model (2) would give a line extending from $3LiF \cdot ThF_4$ toward $BeF_2 - ThF_4$ (60-40 mole %). This is a limiting line which permits considerably higher ThF_4 content than that found experimentally. Accordingly, it appears that both models are simultaneously applicable for the crystallization behavior of $3LiF \cdot ThF_4$ as it crystallizes from $LiF-BeF_2-ThF_4$ melts. Once the crystal structure of $3LiF \cdot ThF_4$ has been established (a study of the structure is currently in progress[6]) it will be possible to appraise the validity of these models.

Application of ternary phase diagrams to technology often requires a knowledge of the identities and compositions of the various phases in equilibrium at specific temperatures. Such information is represented by equilibrium phase diagrams. Typically, phase diagrams of ternary systems are presented as projections of temperature-composition prisms on their basal planes. When such schematic representation includes liquidus temperatures, equilibrium crystallization and melting reactions can be described in a quantitative manner. Here, the use of isothermal sections is often valuable, particularly if the phase diagram is complex. The chief feature of the isothermal section is that it provides information both about the identity and relative masses of coexisting phases.

The crystallization behavior of the $3LiF \cdot ThF_4$ ternary solid solution determines the composition sequence as $LiF-BeF_2-ThF_4$ melts are cooled. A series of equilibrium isotherms is shown in Figs. 2 to 11, which describe all the equilibrium reactions in the temperature interval from $590^\circ C$ to $350^\circ C$, i.e., the liquidus-solidus interval of chief relevance to the compositions which are likely to have application in molten salt reactor technology, and in which all $3LiF \cdot ThF_4$ solid solution melting-freezing reactions occur. Within this interval all the solid phases of the system are involved. The equilibrium behavior of chief importance to us is described further by the temperature-composition sections, $3LiF \cdot ThF_4 - 2LiF \cdot BeF_2$, $LiF \cdot ThF_4 - 2LiF \cdot BeF_2$, and $LiF \cdot 2ThF_4 - 2LiF \cdot BeF_2$, shown in Figs. 12-14 (schematic, not to scale).

Fig. 2.   Isothermal Section of the System LiF-BeF$_2$-ThF$_4$ at 590°C.

Fig. 3.   Isothermal Section of the System LiF-BeF$_2$-ThF$_4$ at 570^{0}C.
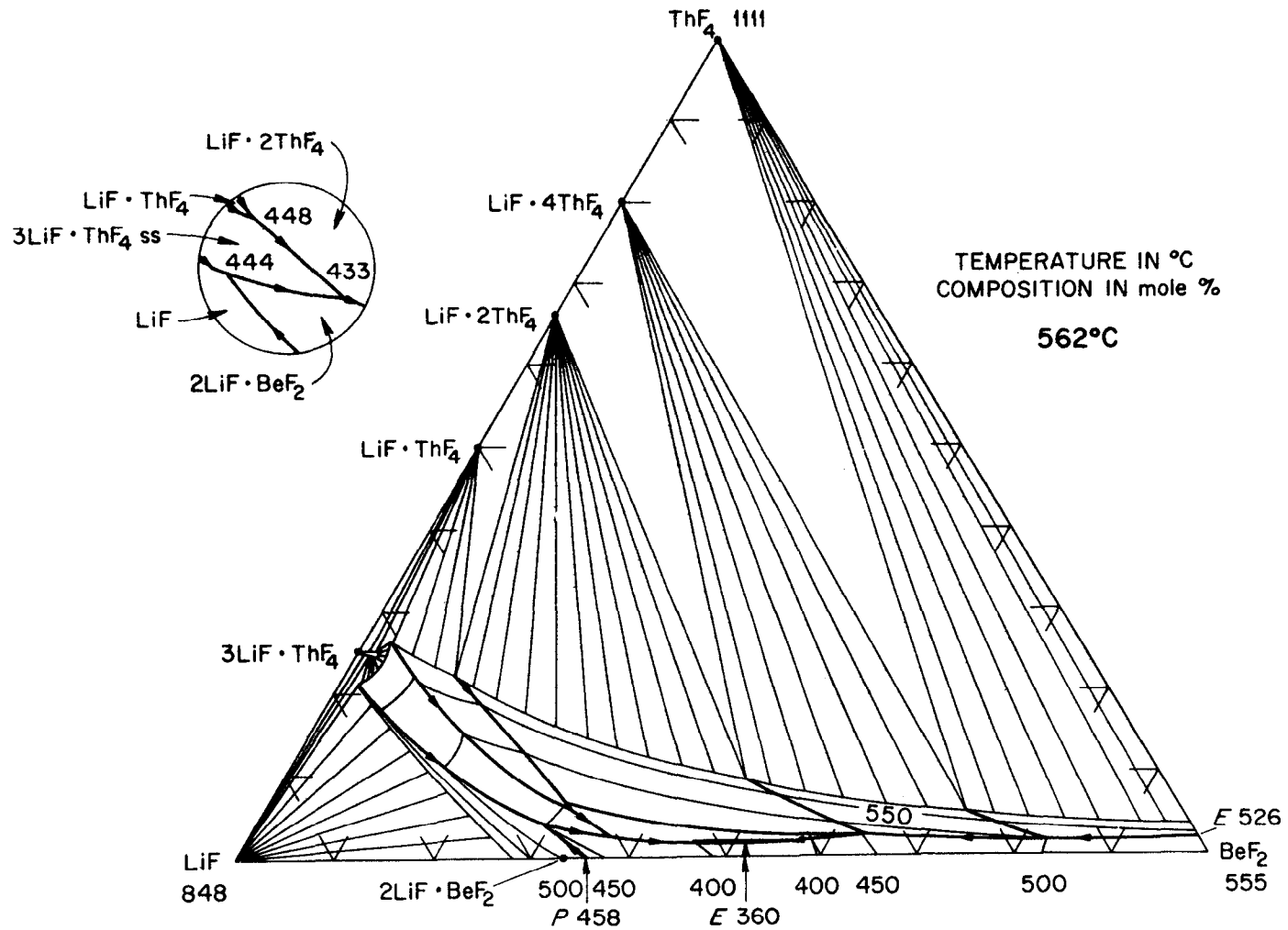
Fig. 4. Isothermal Section of the System LiF-BeF$_2$-ThF$_4$ at 562°C.
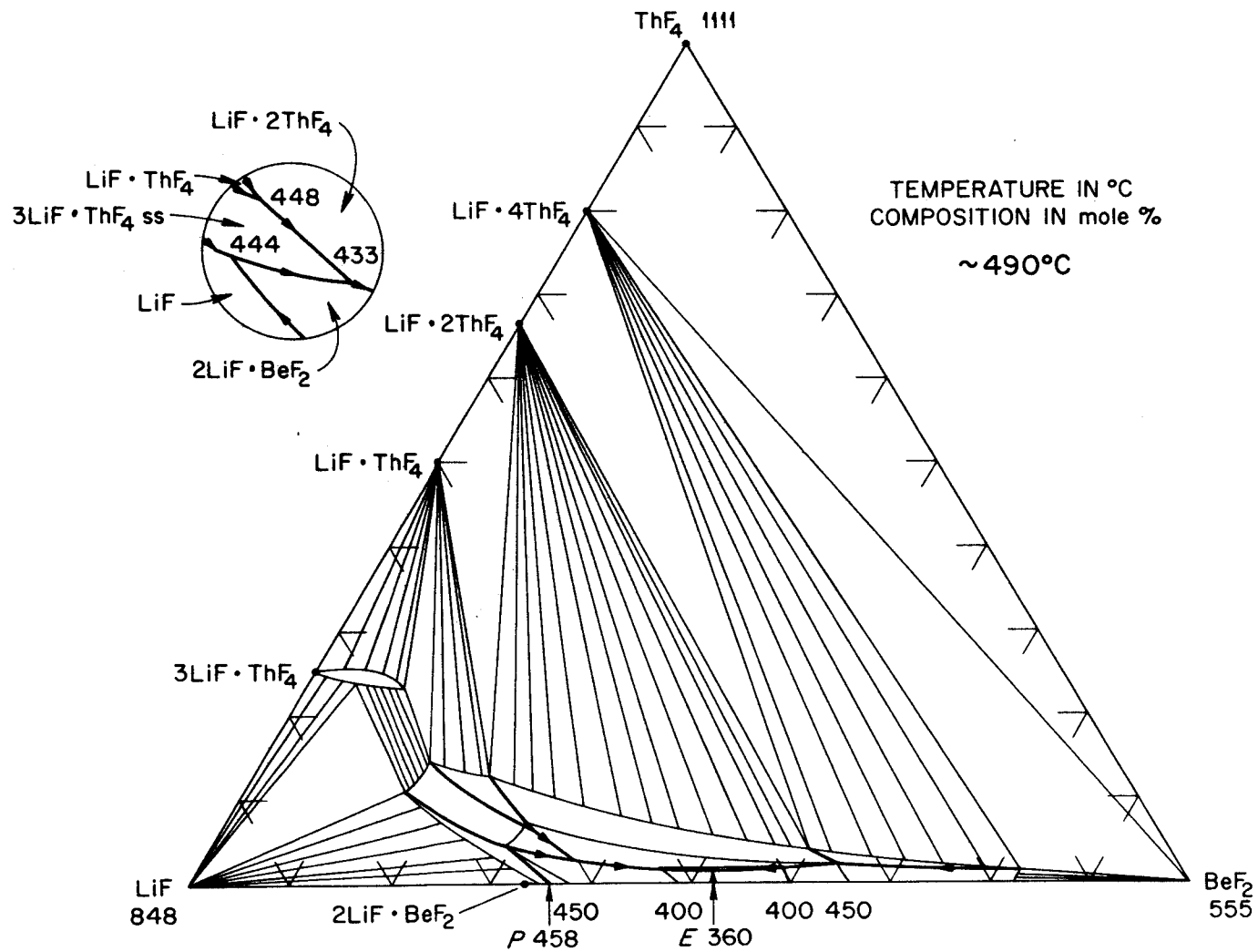
Fig. 5. Isothermal Section of the System LiF-BeF$_2$-ThF$_4$ at 490°C.

ORNL-DWG 68-11680R2
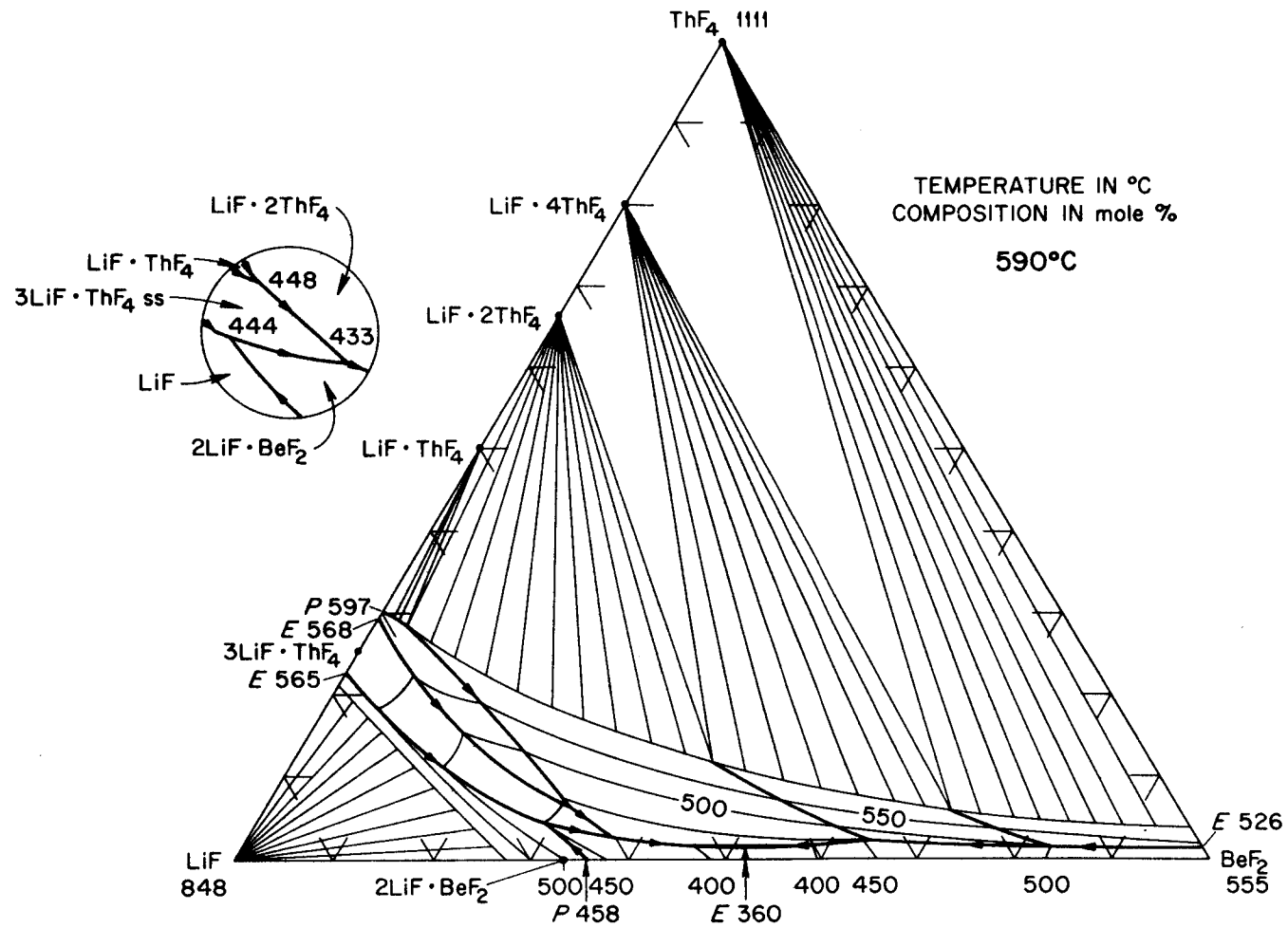
TEMPERATURE IN °C
COMPOSITION IN mole %

457°C

Fig. 6. Isothermal Section of the System LiF-BeF$_2$-ThF$_4$ at 457°C.
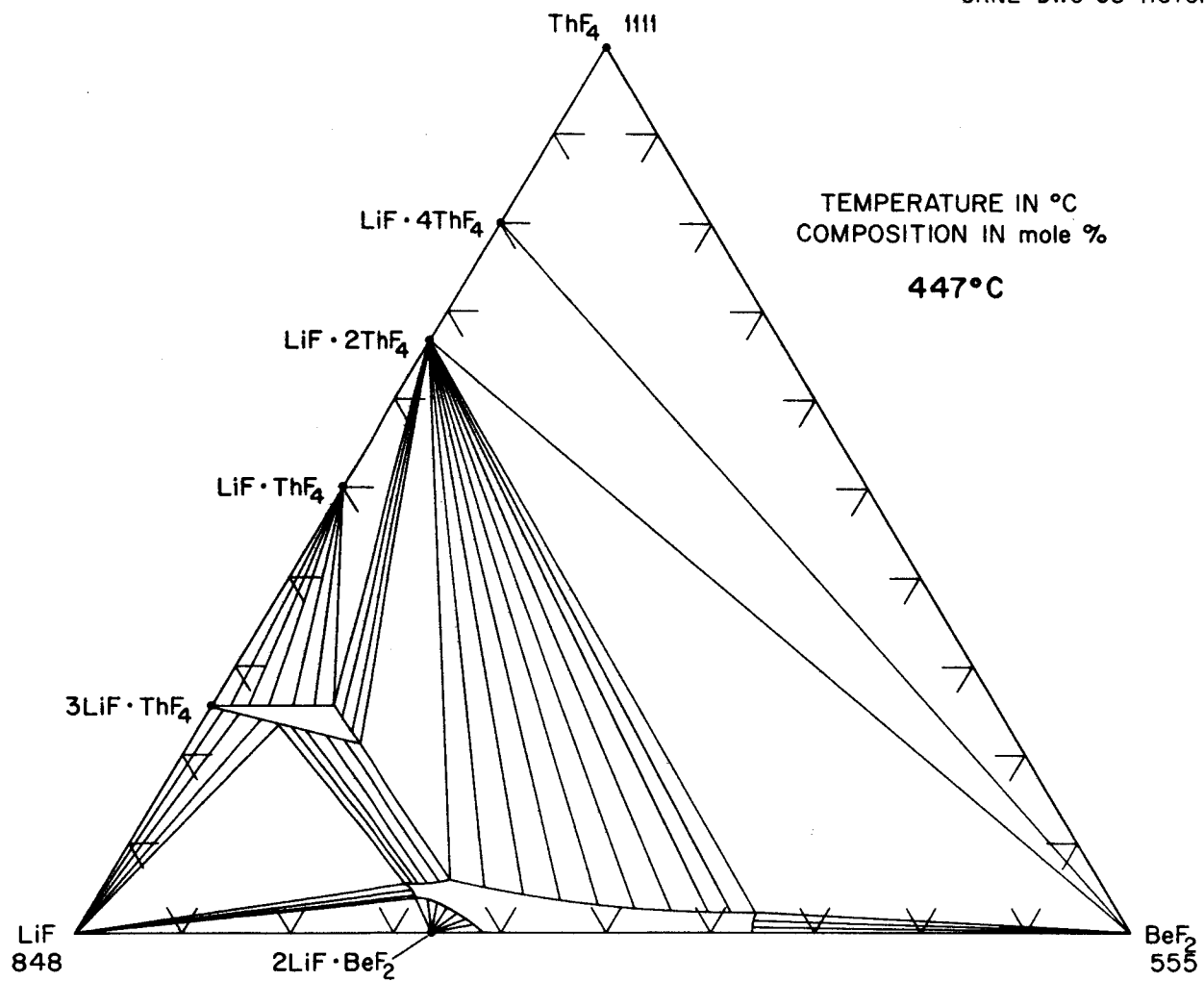
Fig. 7. Isothermal Section of the System LiF-BeF$_2$-ThF$_4$ at 447^{0}C.
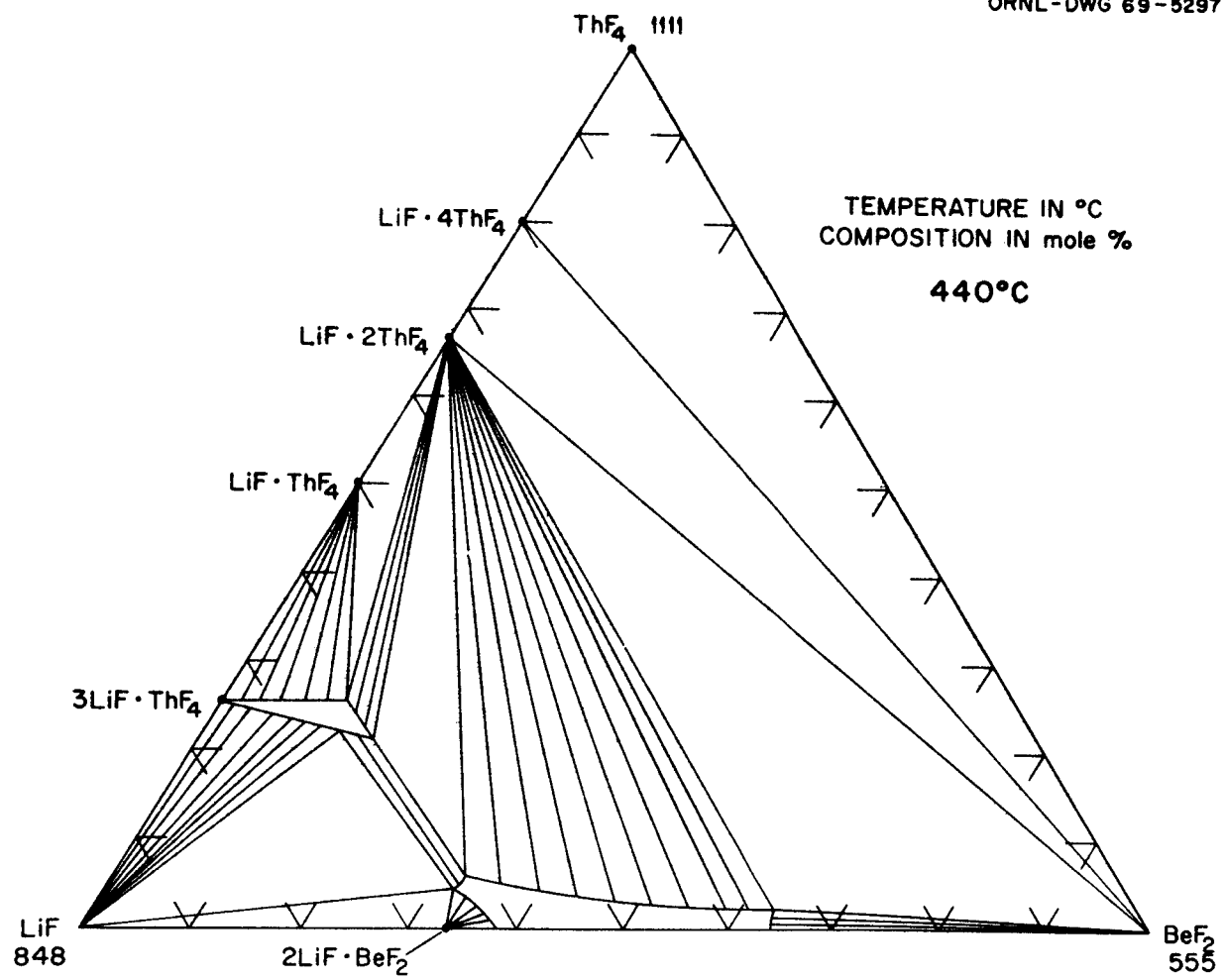
Fig. 8. Isothermal Section of the System $LiF-BeF_2-ThF_4$ at $440^\circ C$.

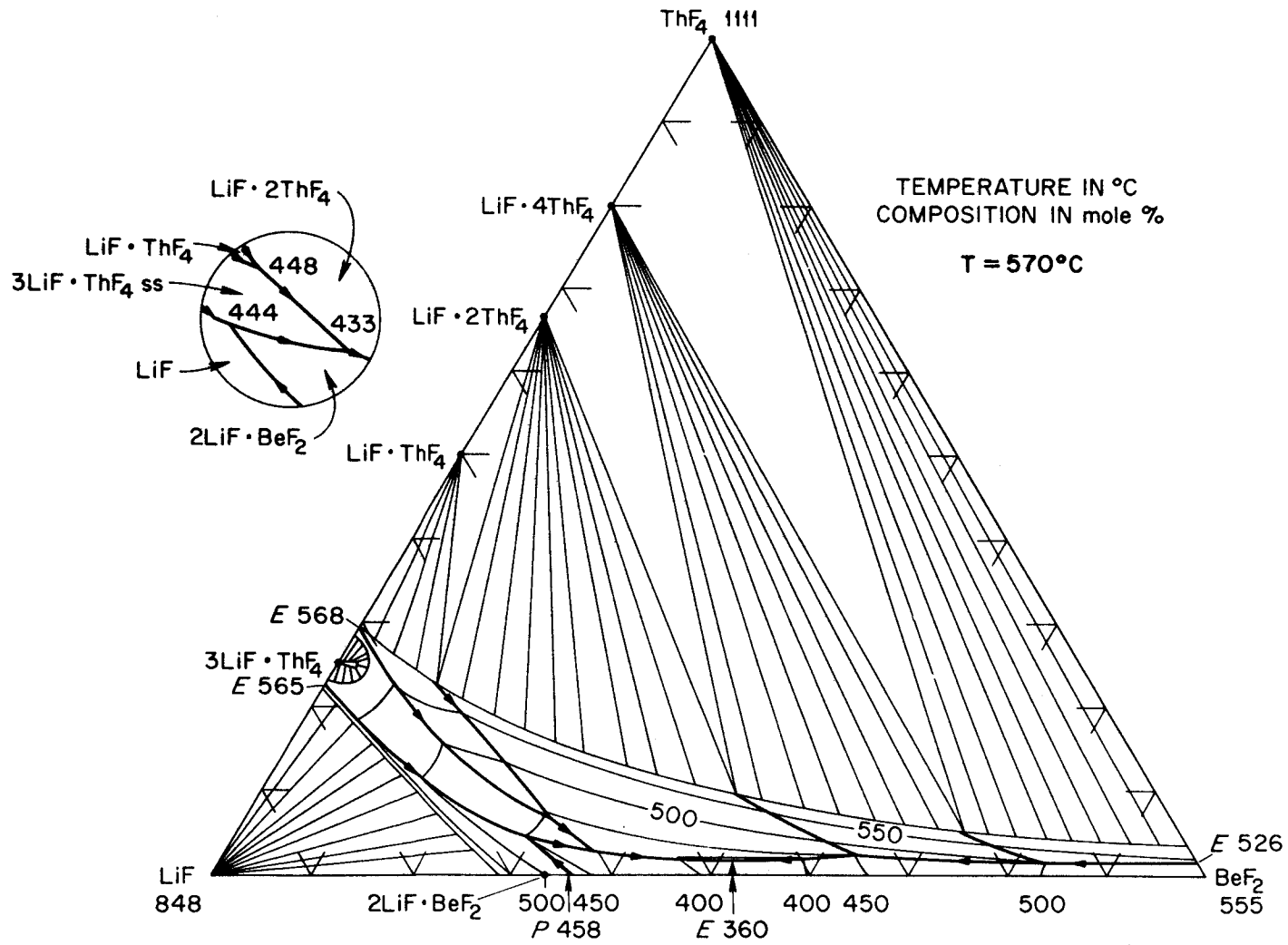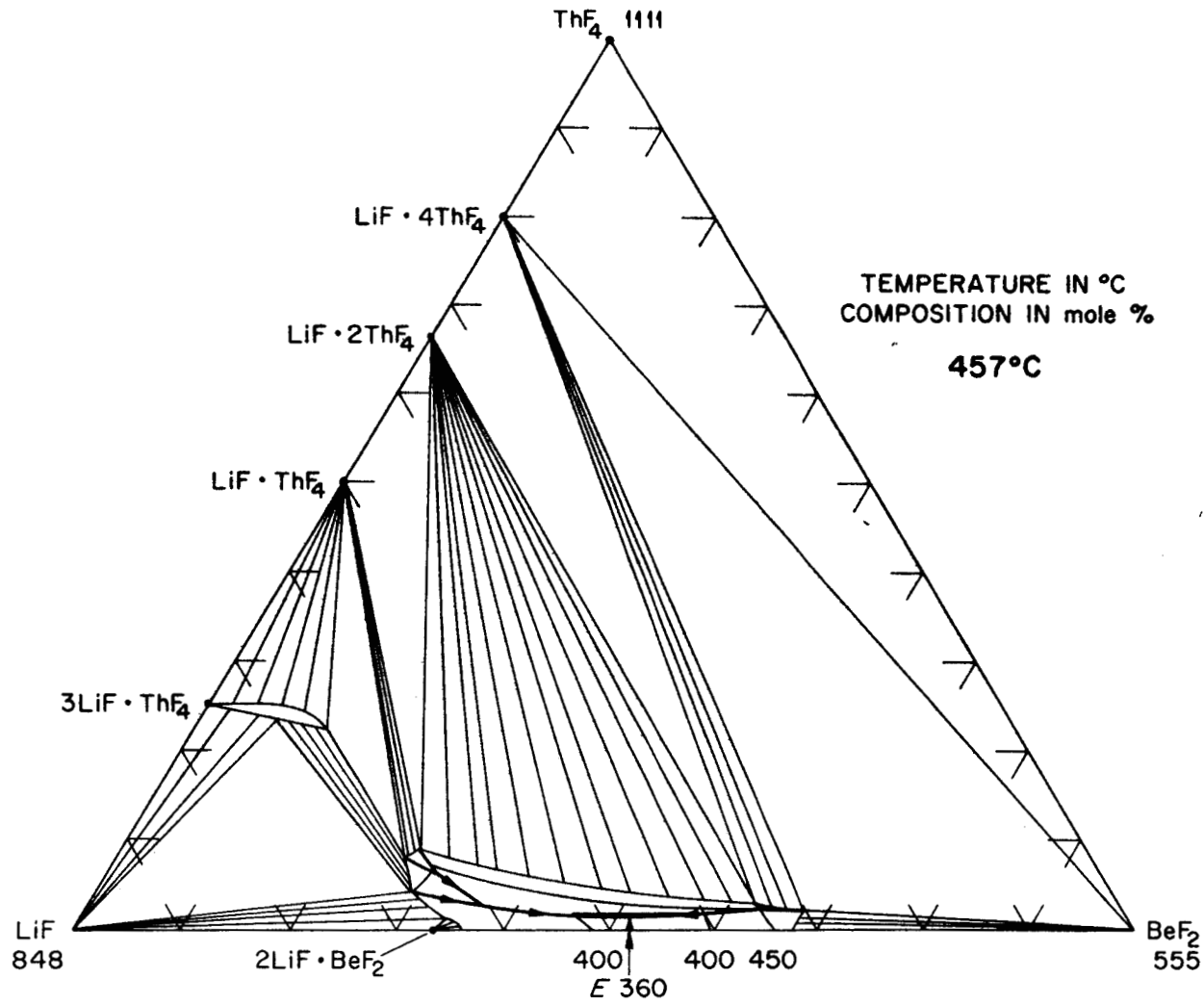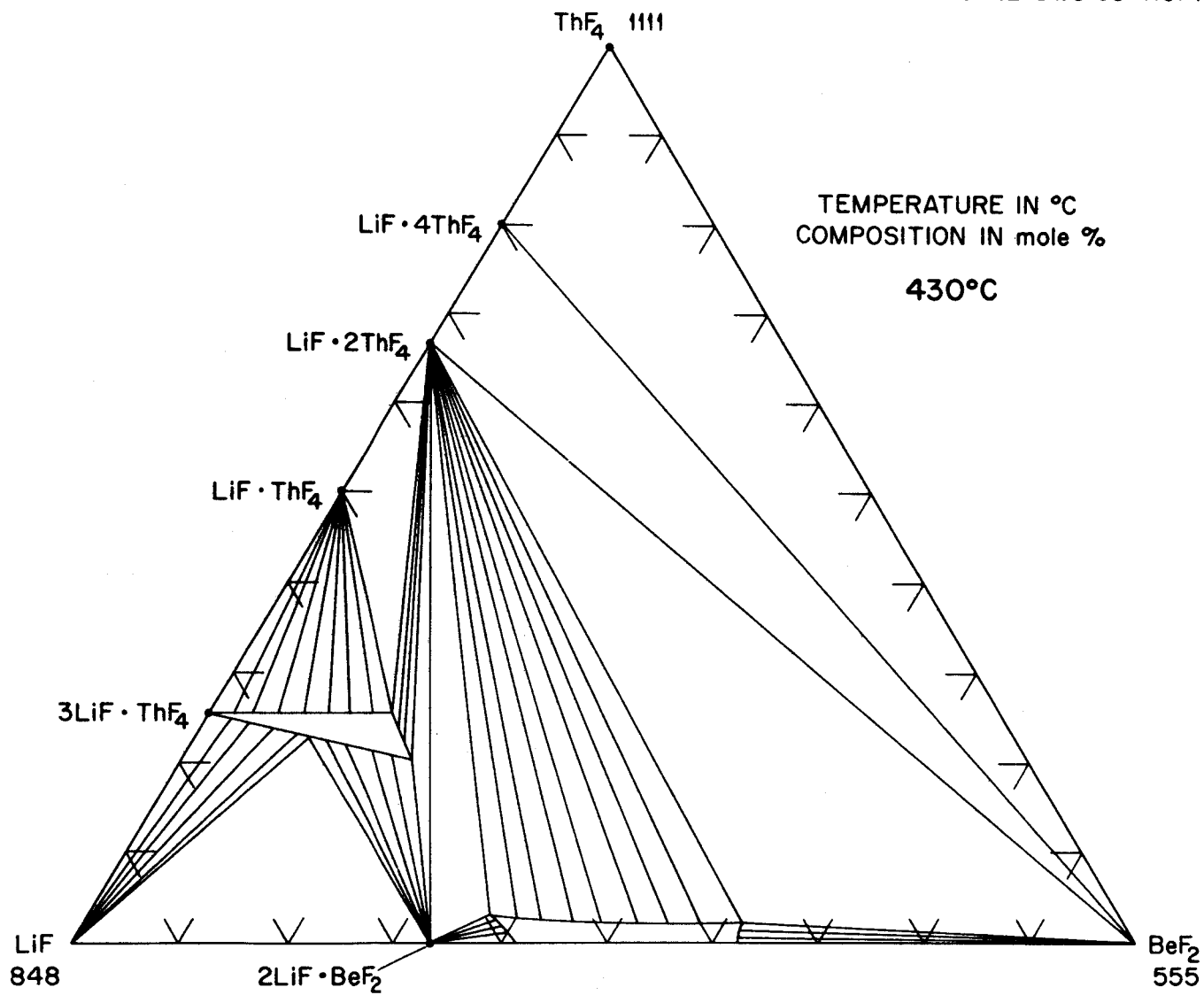Fig. 9.   Isothermal Section of the System LiF-BeF_2-ThF_4 at $430^\circ C$.
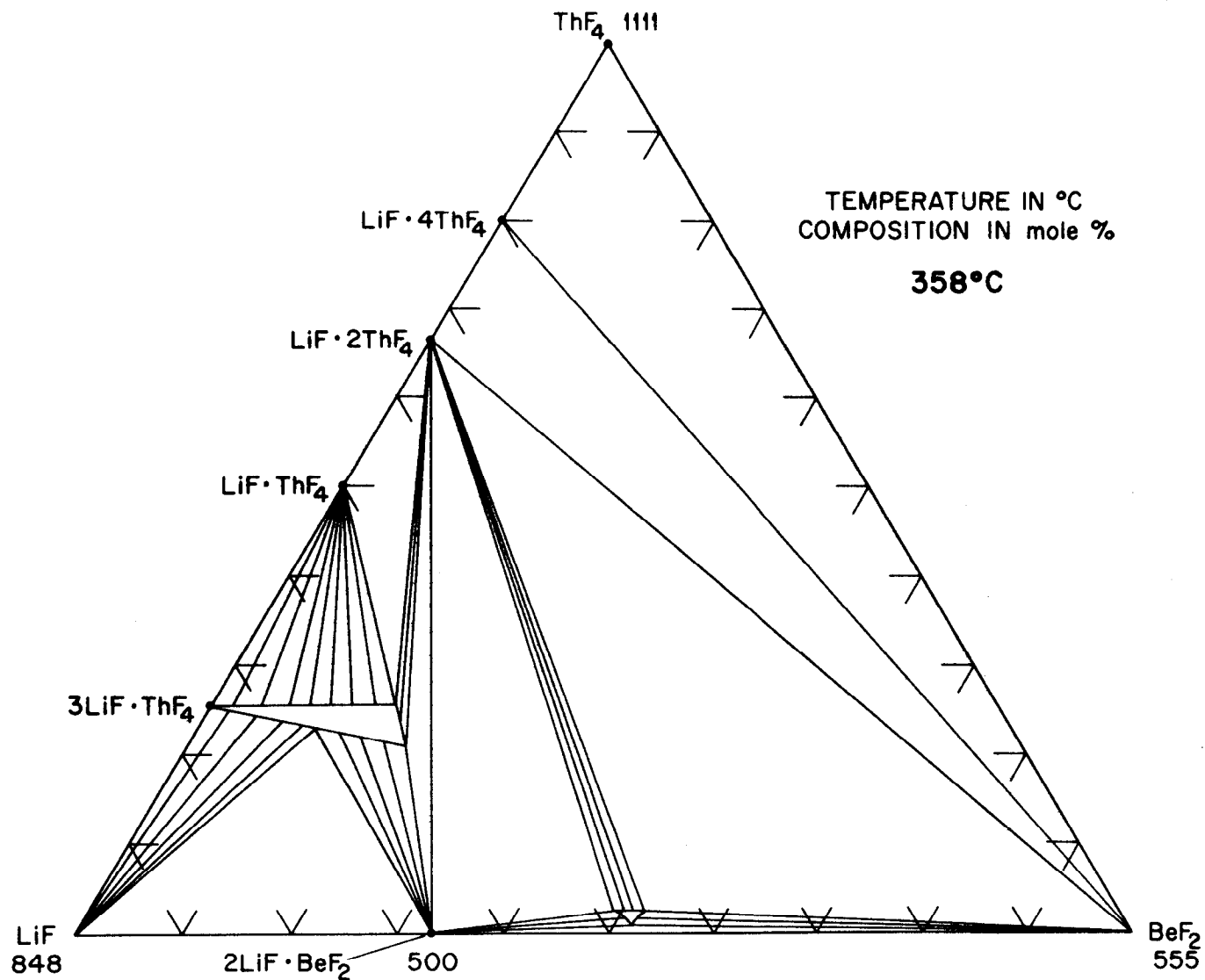
Fig. 10. Isothermal Section of the System LiF-BeF$_2$-ThF$_4$ at 430^{0}C.
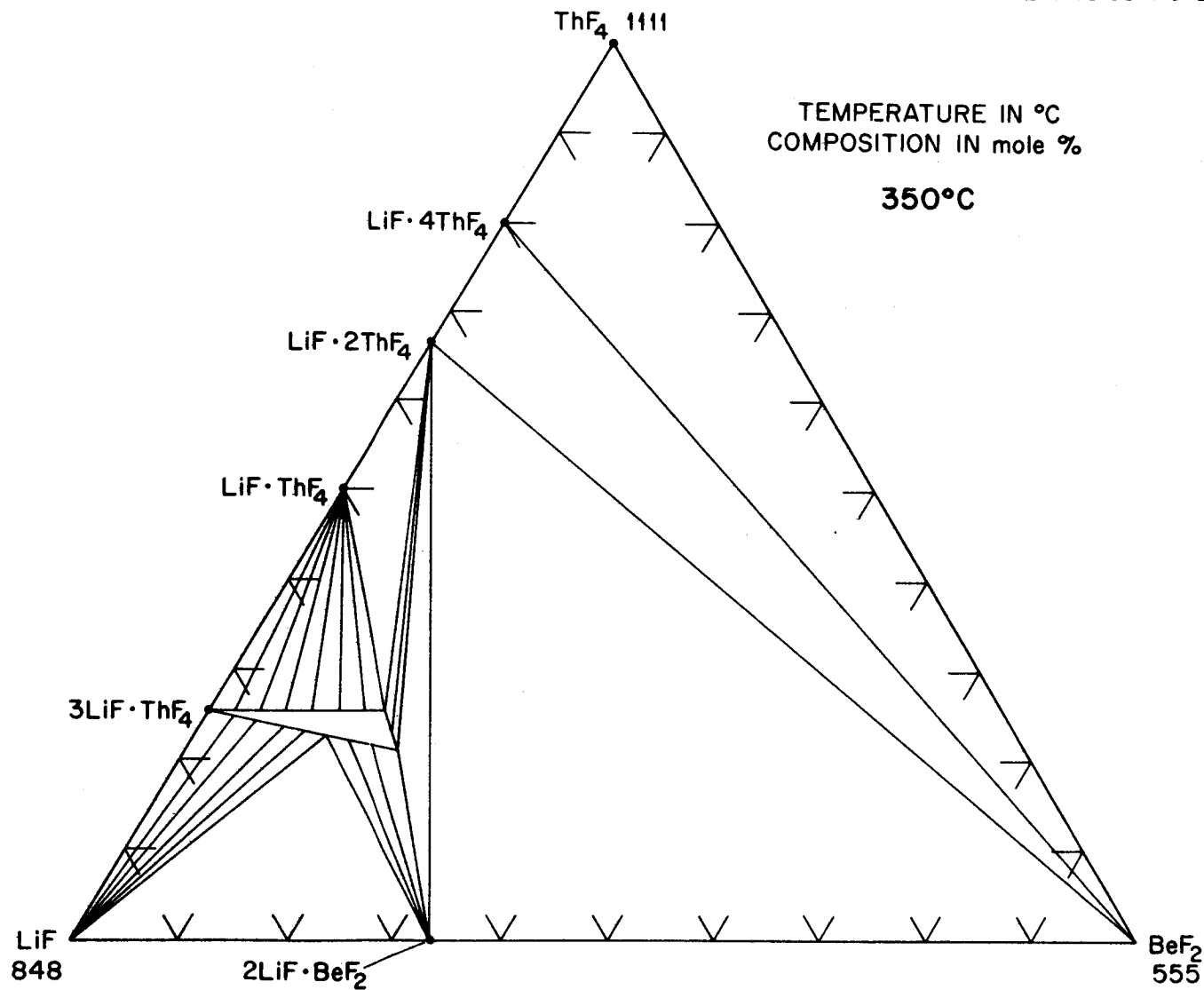
Fig. 11. Isothermal Section of the System $LiF\text{-}BeF_2\text{-}ThF_4$ at $350^{\circ}C$.

The isothermal sections included in Figs. 2 to 11 are drawn to scale and represent the experimental results which were the basis of the previously published phase diagram.[4] Composition-temperature relations in the LiF-BeF$_2$-ThF$_4$ system for LiF concentrations greater than 50 mole % are shown in detail in Fig. 15.

The straight lines appearing in Figs. 2 to 11 are tie-lines (or "conodes") connecting two phases which are in equilibrium. In Fig. 16, point P, as a point on such a tie-line joining points b and z, represents a mixture of the phases (or compositions) b and z with the mole fraction of b equal to the ratio of line lengths zP/zb.

In the case of a mixture of three phases, such as the points a, b, c making up the total composition at point P (Fig. 16), the relative amounts of the phases a, b, c making up P may be determined as follows, with the three fractions defined as x of a, y of b, 1-x-y of c. Then:

(1) Graphically: extend the line bP to fix the point z on the line ac. Then $y = zP/zb$, and $x = (zc/ac)(1-y)$.

(2) Analytically: let the fractions of the components A and B at each of the four points (a, b, c, P) be

$$A_a \quad A_b \quad A_c \quad A_p,$$

$$B_a \quad B_b \quad B_c \quad B_p.$$

Then by similar triangles, we have

$$\frac{B_a - B_z}{A_a - A_z} = \frac{B_a - B_c}{A_a - A_c} = \alpha$$

$$\frac{B_b - B_z}{A_b - A_z} = \frac{B_b - B_p}{A_b - A_p} = \beta$$

Then $B_z = B_b - \beta A_b + \beta A_z = B_a - \alpha A_a + \alpha A_z$

Hence $\quad A_z = \dfrac{(B_a - B_b) + \beta A_b - \alpha A_a}{\beta - \alpha}$

$$B_z = B_b - \beta A_b + \beta(A_z).$$

Then $\quad y = \dfrac{B_p - B_z}{B_b - B_z}$

and $x = \dfrac{A_z - A_c}{A_a - A_c} (1 - y)$.
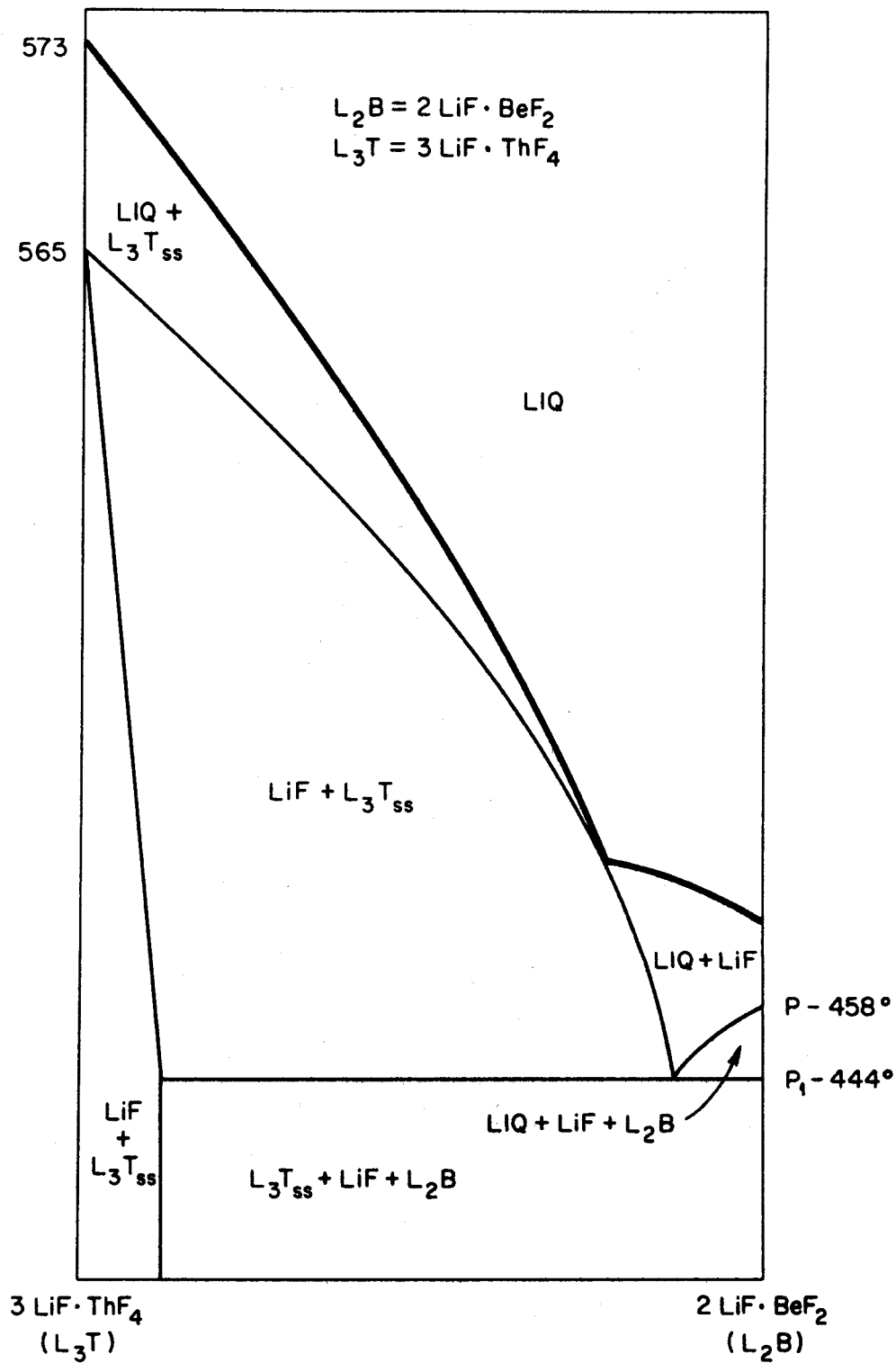
Fig. 12. The Section $3LiF \cdot ThF_4 - 2LiF \cdot BeF_2$

ORNL-DWG 69-5295

LT = LiF · ThF₄
LT₂ = LiF · 2ThF₄
LT₄ = LiF · 4ThF₄
L₂B = 2LiF · BeF₂

LIQ + LT₄

P-762°

LIQ + LT₄ + LT₂

LIQ

LIQ + LT₂

P-597°

LIQ + LT + LT₂

LIQ + LT

LIQ + LT + L₃T_ss

LIQ + L₃T_ss + LiF

LIQ + LiF

P-458°

LIQ + LiF + L₂B

L + L₃T_ss

P-444°

LT + L₃T_ss

LIQ + L₃T_ss + L₂B

P-433°

L₃T_ss

L₃T_ss + L₂B

LiF · ThF₄
(LT)
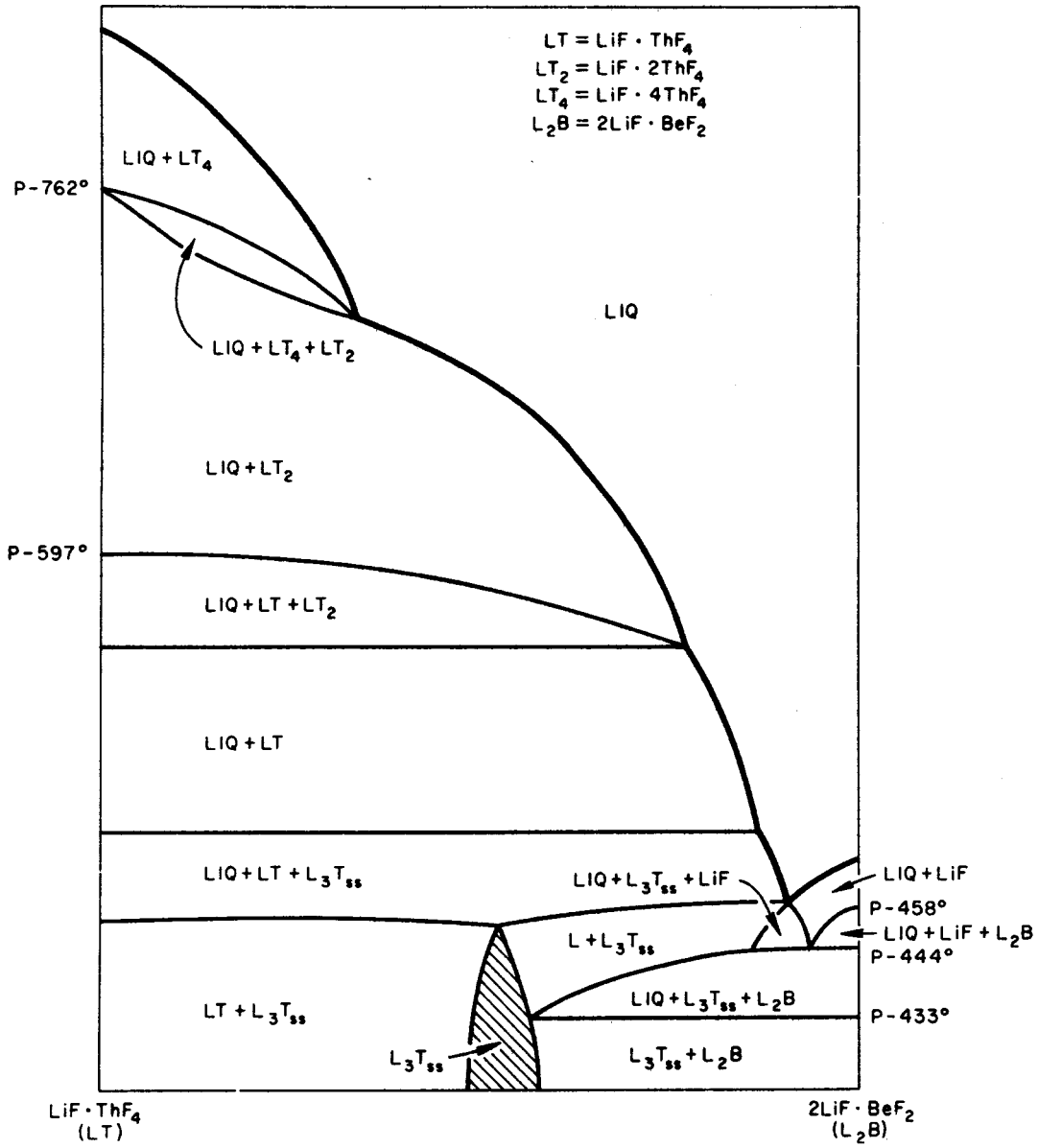
2LiF · BeF₂
(L₂B)

Fig. 13. The Section LiF·ThF₄-2LiF·BeF₂
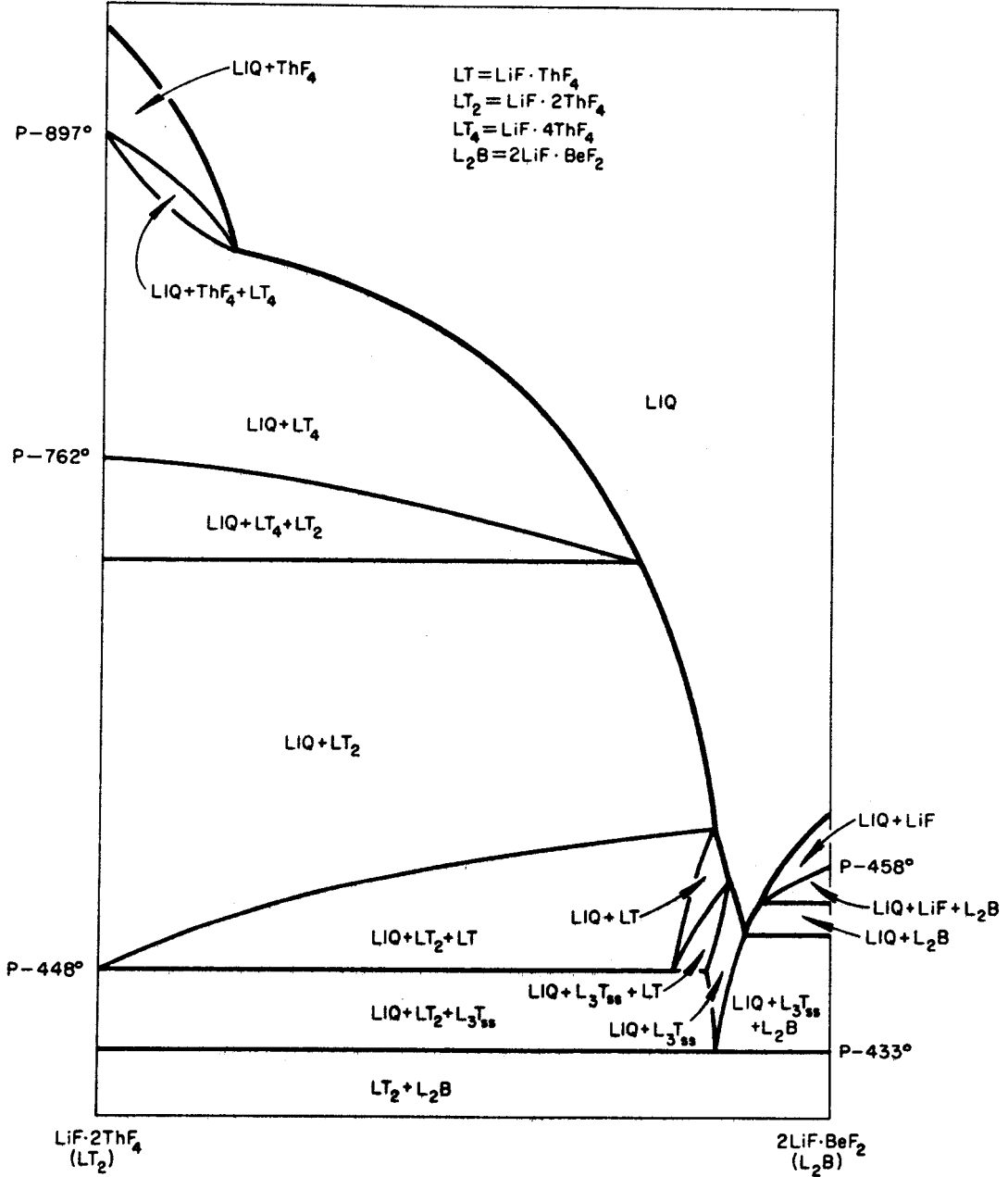
ORNL–DWG 69–5296

Fig. 14. The Section $LiF \cdot 2ThF_4 - 2LiF \cdot BeF_2$

ORNL-DWG 68-942A
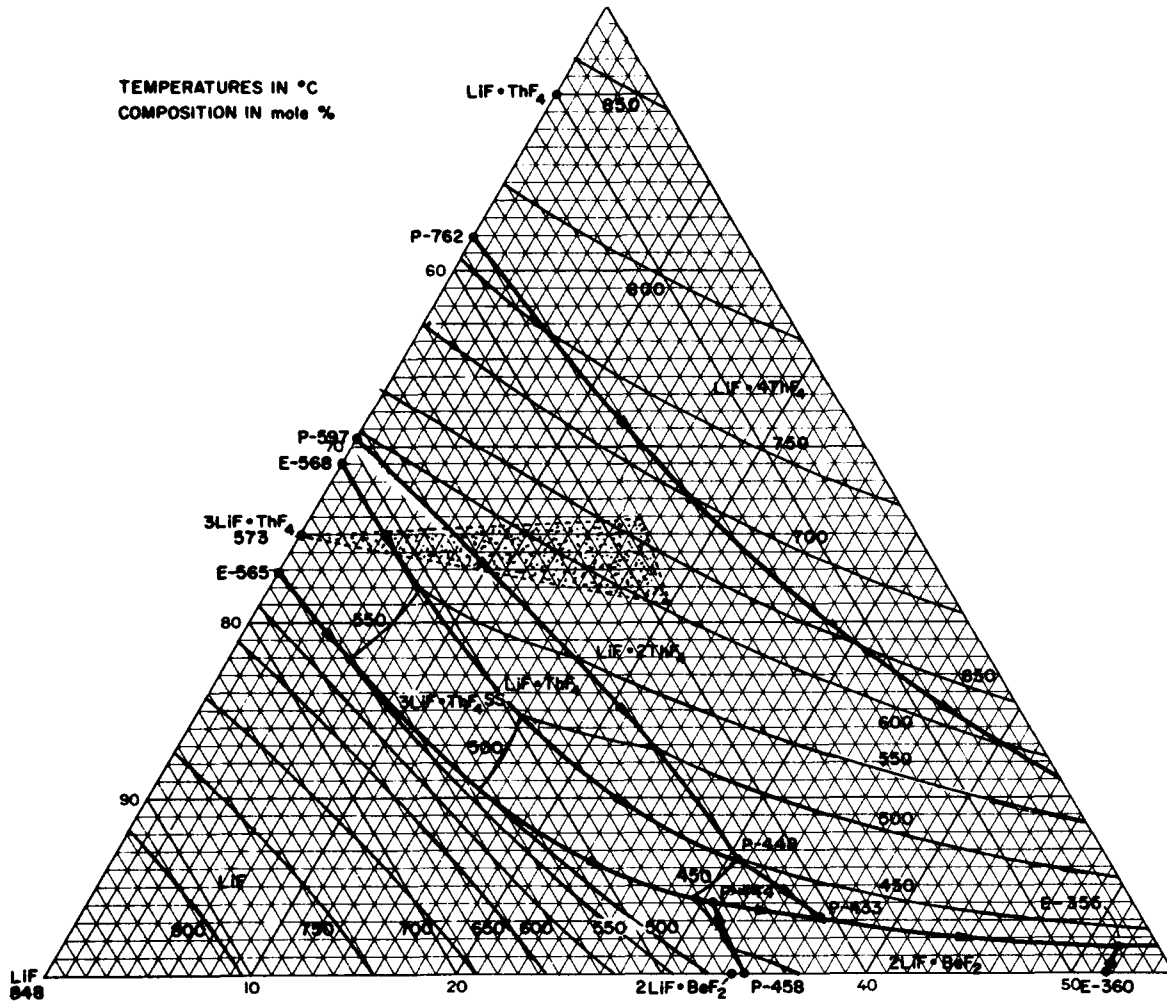
Fig. 15. Phase Diagram of the LiF-BeF$_2$-ThF$_4$ System for Compositions 50 - 100 mole % LiF.

Fig. 16. Schematic Drawing for Use in Calculating Relative Fractions
of Coexisting Phases at Point P.

POTENTIAL APPLICATION OF FRACTIONAL CRYSTALLIZATION

IN CHEMICAL REPROCESSING

Under equilibrium conditions, the crystallization end-point in
three component systems such as in the LiF-BeF$_2$-ThF$_4$ system, depends
on the "compatibility" or three solid phase triangles of the equilibrium
diagram. As an example, compositions in the triangle LiF - 3LiF·ThF$_4$-
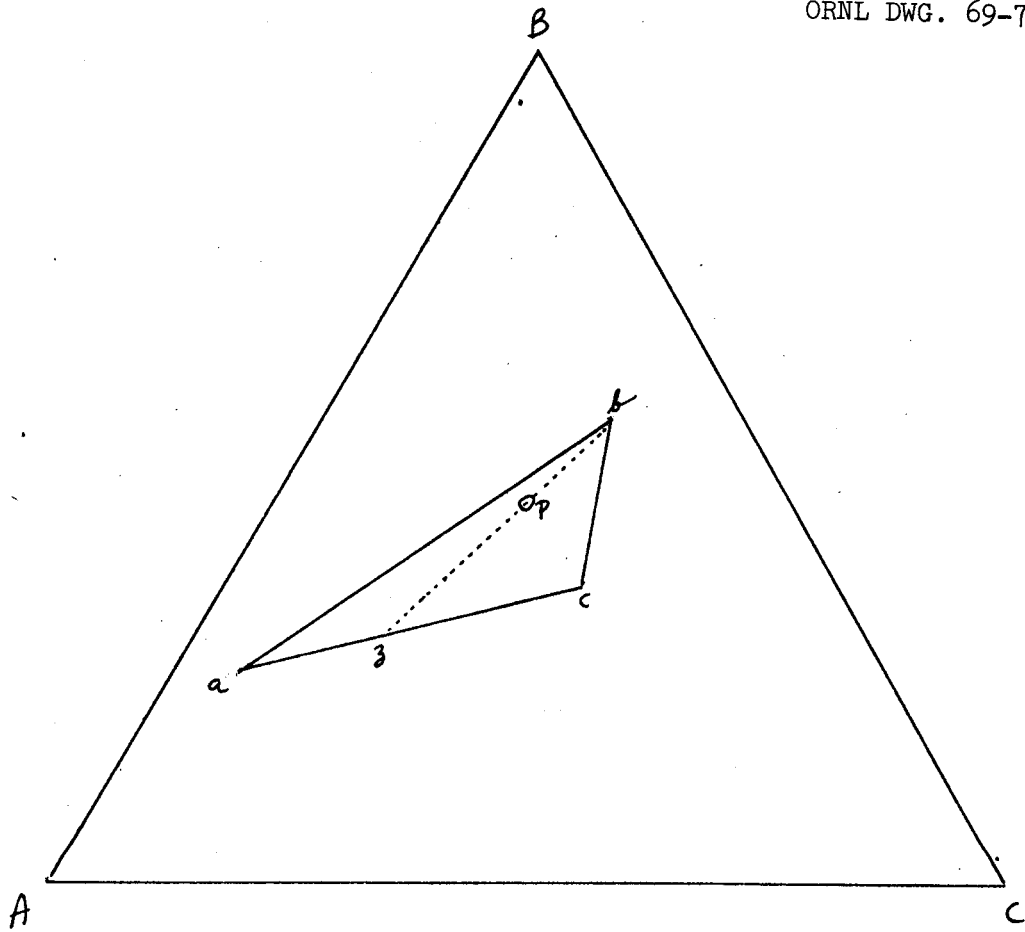2LiF·BeF$_2$ have their crystallization end-point at the 444^{0}C peritectic
reaction point. As noted previously,[7] dynamic crystallization of
LiF-BeF$_2$-ThF$_4$ mixtures does not follow the equilibrium crystallization
diagram exactly; instead, non-equilibrium crystallization proceeds
characteristically by sub-cooling (i.e., delayed crystallization under
dynamic cooling), and by incomplete recombination of liquid and solid
phases at the peritectic reaction points. Thus, liquids are produced
from mixtures which are of interest to us, primarily those containing
high concentrations of LiF, which are richer in BeF$_2$ than their
equilibrium counterparts, and which crystallize as described by the
lower melting areas of the phase diagram. The consequence of non-
equilibrium fractionation is thus to produce liquid residues which are
lower in ThF$_4$ content than at equilibrium.

Let us examine the difference between equilibrium and non-equilibrium
crystallization behavior of a liquid composition that would partially
typify the reactions of MSBR salts. Suppose the composition c, LiF-
BeF$_2$-ThF$_4$ (63-32-5 mole %), undergoes equilibrium crystallization.
On complete solidification, the frozen salt will consist of the three
crystalline phases, 3LiF·ThF$_4$ ss, 2LiF·BeF$_2$ and LiF·2ThF$_4$ in proportions
given by the position of point c in the corresponding triangle of Figs.
9, 10, and 11.

For non-equilibrium crystallization this triangle has no signifi-
cance. The non-equilibrium process consists of four consecutive steps,
seen on the basis of the following diagram:
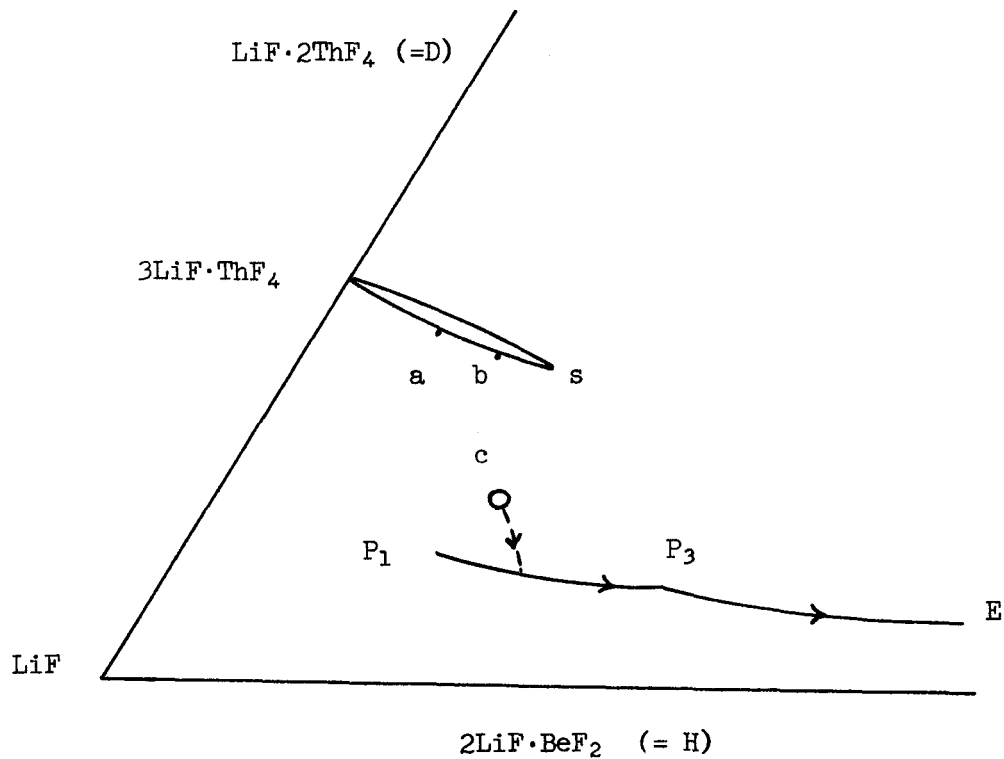
Step (1): freezing starts at ~446°C for composition c, and the liquid travels on the solid solution liquidus surface to reach curve P_1 - P_3 at some point ℓ (at ~440°C), while precipitating some solid solution of composition between a and b, say a' as average.

Step (2): liquid travels on curve P_1-P_3, to reach P_3 (433°C), while precipitating a mixture of solid solution (of composition between b and s, say b' as average) and 2LiF·BeF₂.

Step (3): liquid travels on curve P_3-E, to reach E(356°) while precipitating mixture of LiF·2ThF₄ + 2LiF·BeF₂.

Step (4): liquid at E(356°) freezes to mixture of LiF·2ThF₄ + 2LiF·BeF₂ + BeF₂.

Quantities involved for 1 mole of starting composition c:

Step (1): draw straight line a'c and extend it to curve P_1-P_3, to fix point ℓ:
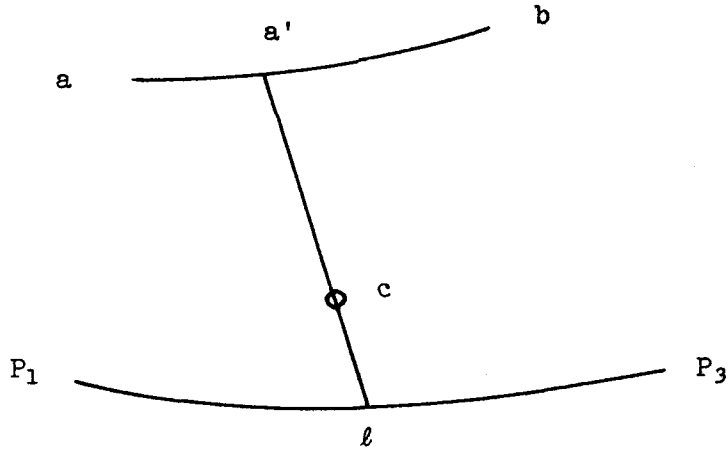
Moles of liquid reaching $\ell = \dfrac{a'c}{a'\ell} = m_1$;

Moles of ThF_4 precipitated (in step 1, or between 446 and 440°)

$$= x_{a'}\,(1-m_1) = p_1,$$

in which $x_{a'}$ = mole fraction of ThF_4 at a', etc.

Step (2): draw straight line b'-H, and extend straight line ℓP_3 back to fix point y on line b'-H:

$2LiF \cdot BeF_2$ (=H)
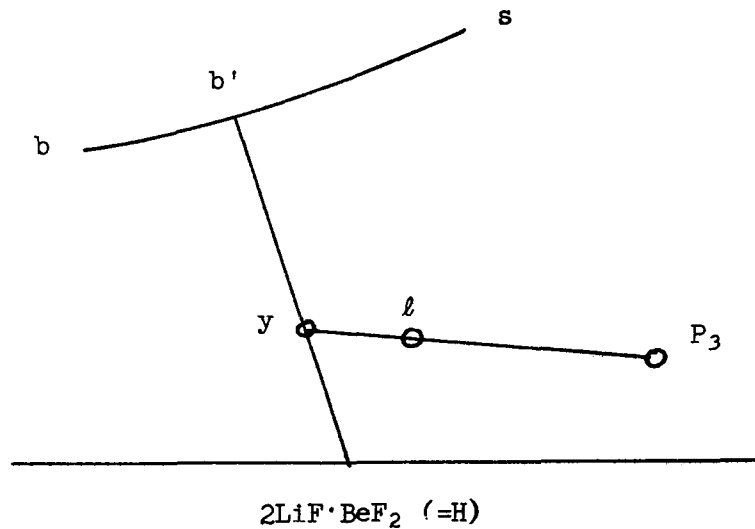
Moles of liquid reaching $P_3 = \dfrac{y\ell}{yP_3}$ $(m_1) = m_2;$

Moles of ThF_4 precipitated (in step 2, or between 440^0 and 433^0)

$$= x_{b'} \frac{yH}{b'H} (m_1 - m_2) = p_2.$$

Step (3): draw straight line DH and extend straight line P_3E back to fix point z on the line DH:

LiF·2ThF$_4$
(=D)

z

P$_3$

E

LiF

2LiF·BeF$_2$ (=H)
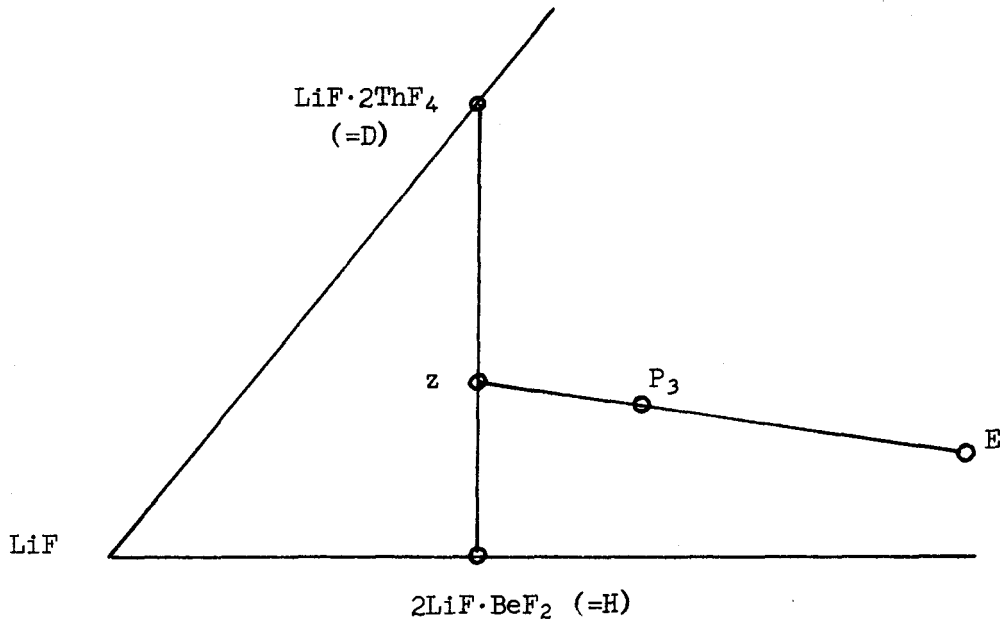
Moles of liquid reaching $E = \dfrac{zP_3}{zE}$ $(m_2) = m_3;$

Moles ThF_4 precipitated (in step 3, or between 433^0 and 356^0)

$$= \frac{2}{3} \left(\frac{zH}{DH} \right) (m_2 - m_3) = p_3,$$

since $x_D = 2/3.$

Step (4): moles ThF_4 precipitated in this step (at 356^0)

$$= x_c - (p_1 + p_2 + p_3).$$

Thus, given the original composition c on the phase diagram as we have it, one can make estimates regarding what happens in steps (1) and (2), and these estimates fix what happens in steps (3) and (4), for the

limit of non-equilibrium behavior. This means a process in which there
is never any interaction between precipitated solid and solution. Actual
behavior will of course be somewhere between this and the equilibrium
process.

Since non-equilibrium fractionation of $LiF-BeF_2-ThF_4$ melts
produces final liquids which are low in thorium, and since the
concentrations of rare earths in the solutions are expected to be about
20 ppm at the time when fuel processing is economically mandatory, one
might anticipate that a semi-zone refining step might well produce
and transport liquids of low thorium concentration and containing a
relatively high concentration of rare earths (the solubility of the
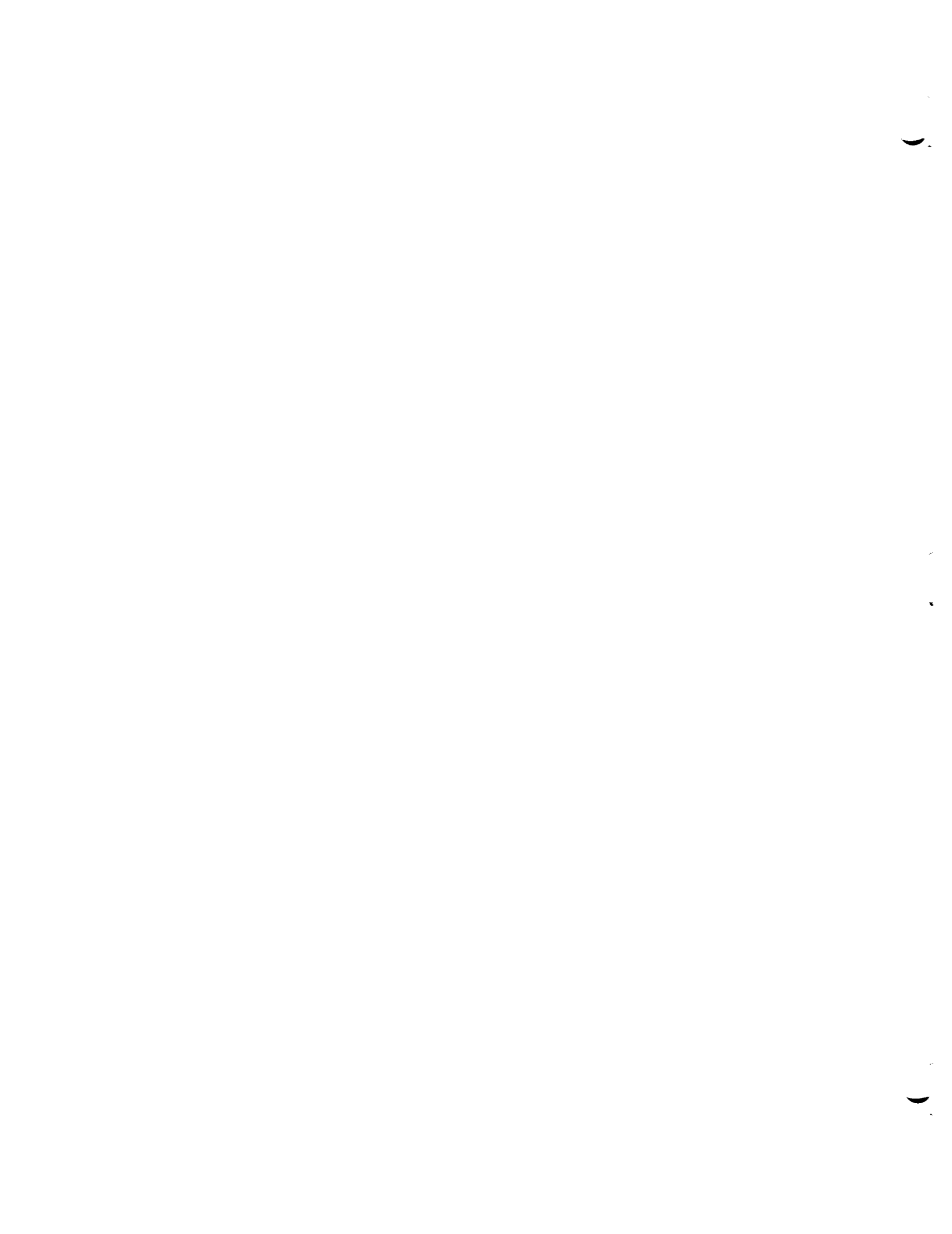lanthanide trifluorides in any of the melts one might encounter is
almost certainly to be at least 200 ppm at the low temperatures which
would be present in this part of the feeder apparatus). The efficiency
of this concentration step could possibly be impaired seriously if the
rare earth trifluorides either formed intermediate compounds (such
compounds are formed only for the lanthanides of $\geq$ 63) which interacted
with the crystallizing phases or otherwise formed solid solutions with
any of the crystallizing phases. The structure of $2LiF \cdot BeF_2$[8] and
$LiF \cdot ThF_4$[9] are known and believed to be incapable of serving as solid
state hosts for the rare earth fluorides. The $3LiF \cdot ThF_4$ solid solution
is an unknown factor in this consideration and could conceivably act as
a solvent for lanthanide ions. This possibility as well as the
possibility that $LiF \cdot 2ThF_4$ might also serve as a solid state solvent
for lanthanide ions could be examined easily through a small scale
laboratory program.

1. Consultant, Department of Chemistry, New York University, University Heights, New York.

2. M. E. Whatley et al., Nuclear Applications, (in press).

3. J. H. Shaffer and D. M. Moulton, Reductive Extraction Processing of MSBR Fuels, in Reactor Chemistry Division Annual Report for Period Ending February 28, 1968, ORNL-4396.

4. R. E. Thoma, H. Insley, H. A. Friedman, and C. F. Weaver, J. Phys. Chem. 64, 865 (1960).

5. J. E. Ricci, Guide to the Phase Diagrams of the Fluoride Systems, ORNL-2396, 1958.

6. G. D. Brunton, ORNL, Unpublished work, 1969.

7. C. F. Weaver, R. E. Thoma, H. Insley, and H. A. Friedman, Phase Equilibria in Molten Salt Breeder Reactor Fuels, I. The System $LiF-BeF_2-UF_4-ThF_4$, ORNL-2896, December, 1960.

8. J. H. Burns and E. K. Gordon, Acta Cryst. 20, 135 (1966).

9. G. D. Brunton, 21, 814 (1964).

DISTRIBUTION

1. R. K. Adams	50. F. L. Culler
2. G. M. Adamson	51. D. R. Cuneo
3. R. G. Affel	52. J. M. Dale
4. J. L. Anderson	53. D. G. Davis
5. R. F. Apple	54. R. J. DeBakker
6. C. F. Baes	55. J. H. DeVan
7. J. M. Baker	56. S. J. Ditto
8. S. J. Ball	57. A. S. Dworkin
9. C. E. Bamberger	58. I. T. Dudley
10. C. J. Barton	59. W. P. Eatherly
11. H. F. Bauman	60. J. R. Engel
12. S. E. Beall	61. E. P. Epler
13. R. L. Beatty	62. D. E. Ferguson
14. M. J. Bell	63. L. M. Ferris
15. M. Bender	64. A. P. Fraas
16. C. E. Bettis	65. J. K. Franzreb
17. E. S. Bettis	66. H. A. Friedman
18. D. S. Billington	67. D. N. Fry
19. R. E. Blanco	68. J. H. Frye, Jr.
20. F. F. Blankenship	69. W. K. Furlong
21. J. O. Blomeke	70. C. H. Gabbard
22. R. Blumberg	71. R. B. Gallaher
23. E. G. Bohlmann	72. R. E. Gehlbach
24. C. J. Borkowski	73. J. H. Gibbons
25. G. E. Boyd	74. L. O. Gilpatrick
26. J. Braunstein	75. W. R. Grimes
27. M. A. Bredig	76. A. G. Grindell
28. R. B. Briggs	77. R. W. Gunkel
29. H. R. Bronstein	78. R. H. Guymon
30. G. D. Brunton	79. J. P. Hammond
31. D. A. Canonico	80. B. A. Hannaford
32. S. Cantor	81. P. H. Harley
33. D. W. Cardwell	82. D. G. Harman
34. W. L. Carter	83. W. O. Harms
35. G. I. Cathers	84. C. S. Harrill
36. J. E. Caton	85. P. N. Haubenreich
37. O. B. Cavin	86. G. M. Hebert
38. J. M. Chandler	87. R. E. Helms
39. F. H. Clark	88. P. G. Herndon
40. W. R. Cobb	89. D. N. Hess
41. H. E. Cochran	90. J. R. Hightower
42. C. W. Collins	91. M. R. Hill
43. E. L. Compere	92. H. W. Hoffman
44. K. V. Cook	93. D. K. Holmes
45. W. H. Cook	94. P. P. Holz
46. J. W. Cooke	95. R. W. Horton
47. L. T. Corbin	96. A. Houtzeel
48. B. Cox	97. T. L. Hudson
49. J. L. Crowley	98. W. R. Huntley

DISTRIBUTION

99.	H. Inouye		148.	T. R. Mueller
100.	W. H. Jordan		149.	H. H. Nichol
101.	P. R. Kasten		150.	J. P. Nichols
102.	R. J. Kedl		151.	E. L. Nicholson
103.	M. T. Kelley		152.	L. C. Oakes
104.	M. J. Kelley		153.	P. Patriarca
105.	C. R. Kennedy		154.	A. M. Perry
106.	T. W. Kerlin		155.	T. W. Pickel
107.	H. T. Kerr		156.	H. B. Piper
108.	J. J. Keyes		157.	B. E. Prince
109.	D. V. Kiplinger		158.	G. L. Ragan
110.	S. S. Kirslis		159.	J. L. Redford
111.	J. W. Koger		160.	M. Richardson
112.	R. B. Korsmeyer		161.	G. D. Robbins
113.	A. I. Krakoviak		162.	R. C. Robertson
114.	T. S. Kress		163.	W. C. Robinson
115.	J. W. Krewson		164.	K. A. Romberger
116.	C. E. Lamb	165-167.	M. W. Rosenthal
117.	J. A. Lane		168.	R. G. Ross
118.	J. J. Lawrence		169.	H. C. Savage
119.	M. S. Lin		170.	W. F. Schaffer
120.	R. B. Lindauer		171.	C. E. Schilling
121.	A. P. Litman		172.	Dunlap Scott
122.	E. L. Long		173.	J. L. Scott
123.	A. L. Lotts		174.	H. E. Seagren
124.	M. I. Lundin		175.	C. E. Sessions
125.	R. N. Lyon		176.	J. H. Shaffer
126.	R. L. Macklin		177.	W. H. Sides
127.	H. G. MacPherson		178.	M. J. Skinner
128.	R. E. MacPherson		179.	G. M. Slaughter
129.	J. C. Mailen		180.	A. N. Smith
130.	D. L. Manning		181.	F. J. Smith
131.	C. D. Martin		182.	G. P. Smith
132.	W. R. Martin		183.	O. L. Smith
133.	H. V. Mateer		184.	P. G. Smith
134.	C. Matthews		185.	I. Spiewak
135.	T. H. Mauney		186.	R. C. Steffy
136.	R. W. McClung		187.	H. H. Stone
137.	H. E. McCoy		188.	R. A. Strehlow
138.	D. L. McElroy		189.	J. R. Tallackson
139.	C. K. McGlothlan		190.	E. H. Taylor
140.	C. J. McHargue		191.	W. Terry
141.	H. A. McLain	192-201.	R. E. Thoma
142.	L. E. McNeese		202.	P. F. Thomason
143.	J. R. McWherter		203.	L. M. Toth
144.	H. J. Metz		204.	D. B. Trauger
145.	A. S. Meyer		205.	W. E. Unger
146.	R. L. Moore		206.	G. M. Watson
147.	D. M. Moulton		207.	J. S. Watson

DISTRIBUTION